Technical Report No. 32-90

A Study of Injection Guidance Accuracy as Applied to Lunar and Interplanetary Missions

H. J. Gordon

jpl

JET PROPULSION LABORATORY
CALIFORNIA INSTITUTE OF TECHNOLOGY
PASADENA, CALIFORNIA
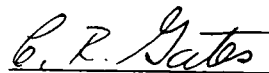
May 15, 1961

Technical Report No. 32-90

A STUDY OF INJECTION GUIDANCE

ACCURACY AS APPLIED TO LUNAR

AND INTERPLANETARY MISSIONS

H. J. Gordon

C. R. Gates, Chief

Systems Analysis Section

CONTENTS

TABLES

FIGURES

A STUDY OF INJECTION GUIDANCE ACCURACY AS APPLIED TO LUNAR AND INTERPLANETARY MISSIONS

H. J. Gordon

ABSTRACT

This report discusses studies that were performed at the Jet Propulsion Laboratory to determine the accuracy of a typical inertial guidance system as applied to future lunar and interplanetary missions. Errors in guidance systems are described and analytical techniques for converting these into injection and target errors are presented. The statistics of injection, target, and midcourse maneuver errors are briefly developed. The determination of midcourse maneuver fuel requirements, which is the primary purpose of the study, is then discussed.

One of the important results of this analysis was an evaluation of the effect of "parking orbits" on injection guidance accuracy. These "parking orbits" (circular satellite coast periods) will be necessary for practical space missions of the near future in order to satisfy various geometrical constraints in an efficient manner. The technique for calculating the injection errors and the effect of the "parking orbit" on these errors is described.

The results of studies of several specific trajectories are presented, illustrating the degree of accuracy that is to be expected for practical deep space missions of the immediate future. It will be seen that "parking orbits" do not necessarily reduce guidance accuracy, and in fact, that there is an optimum coast arc.

I. INTRODUCTION

Guidance is necessary in order to steer a vehicle to injection. The guidance system accomplishes this task by determining vehicle position and velocity with some measuring device and controlling the direction of the thrust vector until the guidance equations are satisfied, at which time thrust is terminated. If the guidance equations are such that all perturbations which are sensed are adequately compensated for, the vehicle will follow the equivalent of a standard trajectory unless the guidance equipment is inaccurate. In this case, the only sources of coordinate errors at injection are component errors, which lead to an incorrect computation of vehicle position and velocity. Since the vehicle's path is corrected to compensate for any error, true or false, which the guidance system measures, the coordinate errors at injection can be set equal to the measurement errors. This approach allows a system to be evaluated even though the specific guidance equations are not known. Nonstandard performance during burning leads to coordinate dispersions, which are not to be

considered as guidance system errors. These coordinate dispersions can be included in the statistical analysis of injection errors, as indicated in Sec. IV.[1]

Guidance system errors can be computed by integrating trajectories with the assumed component errors, or can be derived analytically. This paper derives an analytic method for computing these errors for an inertial guidance system. The analytic method gives a good first-order approximation which is quite adequate for error studies. By the use of this method a study can be carried out much faster, requiring less computer time than would be needed to actually integrate many trajectories.

II. DESCRIPTION OF SYSTEM STUDIED

The guidance system postulated for this study is a vehicle-borne gyro-stabilized inertial platform on which are mounted three mutually perpendicular integrating accelerometers. A digital computer finds vehicle position and velocity and steers to shut-off in such a manner as to compensate for measurable errors in the flight path.

The component error sources considered in this analysis are accelerometer errors and gyro errors. The accelerometer errors are

---

[1]The guidance system attempts to compensate for all dispersions which are sensed. Approximations in the guidance equations may permit some dispersions to be undetected and hence uncorrected. Fuel depletion before desired thrust termination is sensed, but leads to dispersions which cannot be corrected. These dispersion sources may be minimized by proper design of the overall system.

considered to be scale factor, null shift, alignment, and integrator scale factor errors. The gyro errors are considered to be initial offset, random drift, and "g-sensitive" drift. It is assumed that these error sources are uncorrelated. Figure 1 shows the accelerometer orientation, Fig. 2 shows one accelerometer computer loop, Fig. 3 shows the gyro orientation, and Table 1 lists the component errors used for this study. These values were taken from the open literature (1, 2, 3, 4). They represent reasonable values, but do not reflect the performance of any specific system.

The pre-injection trajectory is considered to be divided into two powered flight phases, separated by a circular parking orbit coast period. (See Fig. 4.) The parking orbit will be discussed further in Sec. VI. The coordinate errors contributed by each of the powered flight phases are computed in terms of quantities obtained from the standard trajectory, and the results are combined at injection (See Appendix B). Certain assumptions are made in order to simplify the analysis, such that the vehicle is restricted to a plane (the thrust plane).

III. DESCRIPTION OF THE COMPUTATION

OF INJECTION COORDINATE ERRORS

At entry into the parking orbit the position and velocity errors arising from each error source are computed in an inertial Cartesian coordinate system (the plumb line system defined in Fig. 4) to obtain a six-dimensional error vector. The error vectors are transformed to the downrange point where the final burn terminates by a circular orbit B matrix (See Appendix A). This transformation is most simply carried out if the coordinate errors in the plane of motion are first put into polar coordinates (See Fig. 4). The total coordinate error vectors at injection are then obtained by adding the errors contributed by the final burn and those accumulated during the coast interval.

Error vectors in Cartesian coordinates are designated by $\vec{\delta X_i}$ (the subscript i indicates the number of the error source, of which a total of 18 are considered). The components of $\vec{\delta X_i}$ are designated by δx_{ij}; j taking on the values one through six, corresponding respectively to δX, δY, $\delta \dot{X}$, $\delta \dot{Y}$, δZ, and $\delta \dot{Z}$ which are the displacement and velocity errors defined in the inertial plumb line system. Error vectors in polar coordinates are designated by $\vec{\delta Z_i}$, with elements δz_{ij}, where j takes the values one through six, corresponding respectively to δx, δr, δV, $\delta \Gamma$, δz, and $\delta \dot{z}$. Writing $\vec{\delta X_i}$ and $\vec{\delta Z_i}$ as row vectors, it is convenient to define $[\delta X]$ and $[\delta Z]$ as 18 x 6 matrices with elements δx_{ij} and δz_{ij}.

A $[\delta X]$ matrix is obtained for each of the two burning periods. These are designated $[\delta X]_1$ and $[\delta X]_2$ corresponding to the burnout times t_1 and t_2. The matrices $[\delta Z]_k$ are computed from the transformation matrix E_k by: $[\delta Z]_k = [\delta X]_k E_k$, where E_k is the transformation from Cartesian to polar coordinates at time t_k, $k = 1$ or 2. (See Appendix A.)

The matrix which describes the coordinate errors at injection due to first burn only is $[\delta Z]_{I1} = [\delta Z]_1 B$. For ease of computation, one coordinate error, due to integrator scale factor error, accumulated during the coast interval is calculated directly in polar coordinates. This computation results in a $[\delta Z]_3$ matrix. The total coordinate error matrix at injection is then $A = [\delta Z]_{I1} + [\delta Z]_2 + [\delta Z]_3$. The elements of these matrices are derived in Appendix B.

IV. STATISTICAL CALCULATIONS

The six injection errors are random variables and must be described by a six dimensional probability density function. If each error source is a Gaussian variable, and if a linear relationship exists between these error sources and the injection errors, then the injection error distribution is Gaussian.

An N-dimensional Gaussian distribution can be represented as:

$$f(X_1, X_2, \ldots, X_N) = (2\pi)^{-\frac{N}{2}} \left| \Lambda \right|^{-1/2} \exp\left\{ -1/2 \, \vec{X} \, \Lambda^{-1} \vec{X}^T \right\}$$

where $X_1, \ldots, X_N$ are random variables, $\vec{X} = (X_1, X_2, \ldots, X_N)$, the superscript T indicates the transpose of the matrix with that superscript, and Λ is the moment (or covariance) matrix which is real and symmetric. The elements of the Λ matrix are the ensemble averages of the products of the elements of the X vector.

$$\Lambda = \overset{\sim}{\vec{X}^T \vec{X}} = \begin{bmatrix} \sigma_{x_1}^2 & \rho x_1 x_2 \sigma_{x_1} \sigma_{x_2} & \rho x_1 \rho x_3 \sigma_{x_1} \sigma_{x_3} & \cdots \\ \rho x_2 x_1 \sigma_{x_2} \sigma_{x_1} & \sigma_{x_2}^2 & \rho x_2 \rho x_3 \sigma_{x_2} \sigma_{x_3} & \cdots \\ \vdots & \vdots & \vdots & \\ & & & \sigma_{x_N}^2 \end{bmatrix}$$

where $\sigma_{x_i}^2$ is the variance of the ith random variable,

and $\rho_{x_i x_j}$ is the correlation between the ith and j^{th} random variables.

Thus Λ is a complete statistical description of the probability distribution (5). The moment matrix of error sources, $\Lambda^{(s)}$ on a powered flight trajectory is

$$\Lambda^{(s)} = \begin{bmatrix} \sigma_{s_1}^2 & 0 & 0 & - \\ 0 & \sigma_{s_2}^2 & 0 & - \\ 0 & 0 & \sigma_{s_3}^2 & - \\ - & - & - & \sigma_{s_N}^2 \end{bmatrix}$$

where $\sigma_{s_i}^2$ is the variance of the ith error source $(i = 1, 2, \cdots, N)$. The off-diagonal terms are zero because it is assumed that there is no correlation between error sources. The same technique can be utilized if error sources are correlated, but in practice it is more convenient to use a set of uncorrelated error sources.

Using linear perturbation theory, an error source vector is mapped into an injection error vector by the transformation (using polar coordinates)

$$\vec{\delta q} = \vec{\delta S}\, L = (\delta x, \ \delta r, \ \delta v, \ \delta\Gamma, \ \delta z, \ \delta\dot{z})$$

L is an N x 6 matrix with elements $l_{ij} = \partial q_j / \partial s_i \begin{cases} i = 1, 2, \ldots, N \\ j = 1, 2, \cdots, 6 \end{cases}$

The moment matrix of injection coordinate deviations, $\Lambda^{(I)}$ is then:

$$\Lambda^{(I)} = \overbrace{\vec{\delta q}^T \vec{\delta q}} = L^T \overbrace{\vec{\delta S}^T \vec{\delta S}}\, L = L^T \Lambda^{(s)} L$$

The A matrix, defined in Sec. III corresponds to $\vec{\delta S}\, L$ where the elements of $\vec{\delta S}$ are the one-sigma values of component errors. Then $A^T A = \Lambda^{(I)}$. It may be desired to add more error sources to the analysis, or to include the effects of coordinate dispersions. This can be done as follows:

$$\text{Let } A^* = \begin{bmatrix} A \\ \Delta \end{bmatrix}$$

where Δ is an (N-18) x 6 matrix containing the additional terms to be included in the analysis. Then $\Lambda = A^{*T} A^*$ is the required covariance matrix. Notice that $A^{*T} A^* = A^T A + \Delta^T \Delta$.

If the U matrix maps injection errors into target errors,

$\vec{\delta M} = \vec{\delta q} \, U = (\delta M_1, \delta M_2, \delta M_3)$. U is a 6 x 3 matrix with elements

$$u_{ij} = \partial M_j / \partial q_i; \quad \begin{matrix} i = 1, 2, \ldots, 6 \\ j = 1, 2, 3 \end{matrix}$$

The moment matrix of target errors is then:

$$\Lambda^{(M)} = \widetilde{\vec{\delta M}^T \, \vec{\delta M}} = U^T \, \Lambda^{(I)} \, U$$

The elements of M may be position deviations at a standard time or at closest approach, or other quantities of interest such as relative velocity or time of flight at closest approach.

The U matrix may be considered as a function of the initial and final values of some parameter defining position on the standard trajectory. The initial value refers to the point where $\vec{\delta q}$ is evaluated and the final value to the point where $\vec{\delta M}$ is evaluated. For convenience, consider the final point fixed, as in the paragraph above where we have defined $\vec{\delta q}_{(I)} \, U(I, T) = \vec{\delta M}$, I indicates injection, and T indicates the reference position at the target. If a midcourse maneuver is to be made, it will be made at some point C on the trajectory. At that point, $\vec{\delta q}_{(C)} \, U(C, T) = \vec{\delta M}$. The midcourse maneuver changes the velocity such that all or some of the components of $\vec{\delta M}$ are nulled.

The midcourse velocity maneuver required is then (6)

$$\vec{\delta q}_v = - \vec{\delta M} \, F$$

where F is a 3 x 3 matrix with elements

$$f_{ij} = \partial M_j / \partial \dot{q}_i; \begin{cases} i = 1, 2, 3 \\ j = 1, 2, 3 \end{cases}$$

such that the velocity components are expressed in the appropriate coordinate system.

The moment matrix of midcourse velocity requirements is then:

$$\Lambda^{(v)} = \widetilde{\delta q_v^T q_v} = F^T \Lambda^{(M)} F$$

The amount of fuel necessary to perform the midcourse maneuver may then be calculated.

V. UNITS OF VARIANCE

To determine the effect of each component error, the uncorrected RMS value of the magnitude of the change in impact parameter, which is the distance from the center of the target to the incoming asymptote, was used as a figure of merit, FOM (7). The components of this FOM are represented by the elements of $\vec{\delta M}$ which have been developed above.

$$\vec{\delta M} = \vec{\delta S} \, LU = \vec{\delta S} D$$

where D = LU

The elements of D are $d_{ij} = \dfrac{\partial M_j}{\partial s_i} \begin{cases} i = 1, 2, \ldots, N \\ j = 1, 2, 3 \end{cases}$

$$\mathrm{FOM}^2 = \left|\overrightarrow{\delta M}\right|^2 = \delta M_1^2 + \delta M_2^2 + \delta M_3^2 = \sum_{k=1}^{3} \sum_{i,j=1}^{N} \frac{\partial M_k}{\partial s_i} \frac{\partial M_k}{\partial s_j} s_i s_j$$

$$= \sum_{k=1}^{3} \sum_{i=1}^{N} \left(\frac{\partial M_k}{\partial s_i}\right)^2 \sigma_{s_i}^2 = \sum_{i=1}^{N} p_i^2 \sigma_i^2$$

where

$$p_i^2 = \left(\frac{\partial M_1}{\partial s_i}\right)^2 + \left(\frac{\partial M_2}{\partial s_i}\right)^2 + \left(\frac{\partial M_3}{\partial s_i}\right)^2$$

The percentage of FOM^2 due to the ith error source, to be called the number of units of variance is

$$n_i = \frac{100 p_i^2 \sigma_i^2}{\mathrm{FOM}^2}$$

The value of the ith error source which produces one unit of variance is

$$u_i = \frac{\mathrm{FOM}}{10 p_i}$$

Values of n_i are listed in Table 2 for the trajectories studied.

VI. EFFECT OF PARKING ORBIT

Direct ascent trajectories lose payload rapidly as true anomaly at injection increases. In order to satisfy the necessary geometrical constraints and avoid large payload losses, the launching location must be moved. This is an impractical solution. By using a parking orbit as part of the ascent trajectory, the launcher is effectively moved and a given mission may be accomplished with a resulting greater payload. In addition to this primary argument for the use of parking orbits, their utilization affords a simple mechanism of correcting for launch time delays (8). Thus it appears that a parking orbit will be used for most lunar and interplanetary missions.

A study was made to determine the effect of the parking orbit interval on guidance errors. The parking orbit determines the effects of the errors due to the first burning phase. The second burning phase errors, in polar coordinates, do not change for a given mission. This illustrates the utility of the polar coordinate system for the near Earth part of the trajectory. For a given parking orbit, the ascent trajectory does not change significantly with launch time delay so that $[\delta Z]_1$ may be considered constant. Then the moment matrix at injection into the parking orbit, $\Lambda^{(1)} = [\delta Z]_1^T [\delta Z]_1$ is also constant. To determine the effect of the parking orbit on the injection errors:

$$\Lambda^{(I)} = A^T A = \left\{ [\delta Z]_1 B + [\delta Z]_2 \right\}^T \left\{ [\delta Z]_1 B + [\delta Z]_2 \right\}$$

$$= [\delta Z]_2^T [\delta Z]_2 + B^T \left\{ [\delta Z]_1^T [\delta Z]_1 + [\delta Z]_1^T [\delta Z]_2 B^{-1} + B^{-1^T} [\delta Z]_2^T [\delta Z]_1 \right\} B$$

$$= \Lambda^{(2)} + B^T \left[\Lambda^{(1)} + \Lambda^{(1,2)} + \Lambda^{(1,2)T} \right] B$$

where $\Lambda^{(2)} = [\delta Z]_2^T [\delta Z]_2$ is the contribution of the second burn phase.

$\Lambda^{(1,2)} = [\delta Z]_1^T [\delta Z]_2 B^{-1}$ is a matrix in the form of a sum of outer

products of error vectors due to first burn and those of second burn

rotated back around the coast arc to the point of injection into the parking

orbit. The effect of the parking orbit on guidance accuracy is through the

correlations between injection errors which are seen to be functions of

the coast arc, through the B matrix.

When the post-injection trajectory is determined, launching from a

given location at a certain time requires a definite coast arc in the parking

orbit. For purposes of studying the effect of the parking orbit, it was

assumed that the coast arc could be continuously varied for a given mission.

This implies moving the launcher location. As pointed out above, such an

implication is unrealistic, but it does point out the effects which are caused

by the parking orbit. Another way to change the coast arc would be to launch

at a different date, but this requires a different post-injection trajectory,

and the effect of the coast interval would not be as clearly seen.

VII. RESULTS

The technique described has been used to determine the FOM for several representative lunar and interplanetary missions. Table 3 describes the trajectories and the FOM associated with each of them for the system described in Sec II with the component errors listed in Table 1. The flow chart of computations performed is shown in Fig. 5.

Figure 6 presents FOM versus coast arc in the parking orbit, ψ , for the interplanetary trajectories and Fig. 7 for the lunar trajectories. It is clear that there is an optimum value of the coast arc. This is because correlations between coordinate deviations change as a function of the parking orbit interval, and certain errors may cancel each other. Table 4 lists the standard deviations in polar coordinates and the correlation coefficients for the slow lunar trajectory. Data for the other six trajectories are similar.

Figure 8 presents the FOM versus flight time for the three lunar trajectories. These trajectories impact at roughly the same time, thus having similar geometrical properties. It is seen that the faster trajectories tend to have smaller target error (but, see Fig. 7 where there is a reversal for a coast arc greater than 132 deg). A similar conclusion would be reached for the interplanetary cases. This does not mean that a larger midcourse maneuver would necessarily be required on the slower trajectories, for the higher error sensitivities mean that less correction is required for a given error.

As seen in Appendix B, the values of some of the error terms depend on certain parameters; specifically accelerometer erection angle, ϕ, and gyro orientation angles, α and β. These parameters were varied for the fast Venus trajectory, and the results are shown in Fig. 9.

VIII. CONCLUSIONS

It is seen from Table 2 that of all the error sources considered, only a few are of major significance. Any improvement in the design of the other components would not improve guidance accuracy much if the major error sources were unimproved.

As shown in Figs. 6 and 7 there is an optimum value of coast arc which minimizes the effects of guidance component errors. By scheduling launches appropriately, trajectories could be designed that would utilize near optimum coast arc. Other considerations, such as post-injection trajectory characteristics determined by the positions of the planets will normally determine the scheduling of a launch. The value of the parking orbit study is that it shows that longer coast intervals do not necessarily require larger midcourse maneuver capabilities.

As shown in Fig. 9, there is an optimum set of values for the guidance parameters, α, β, and ϕ. This figure applies to a specific trajectory, but a similar result would apply to other trajectories. The method developed in this paper may be used to evaluate the guidance parameters for any specific trajectory.

TABLE 1

ONE-SIGMA COMPONENT ERRORS (ASSUMING GAUSSIAN DISTRIBUTION)

k	Description			σ_k
1	A	Accelerometer Scale Factor Error		5×10^{-4}
2	B	"	" " "	5×10^{-4}
3	A	"	Null Shift	4×10^{-3} m/sec^2
4	B	"	" "	4×10^{-3} m/sec^2
5	C	"	" "	4×10^{-3} m/sec^2
6	A	"	Alignment Error	0 (See Note #1)
7	B	"	" "	4×10^{-4} radian
8	C	"	" "	4×10^{-4} radian
9	Gyro No. 1		Initial Offset	5×10^{-4} radian
10	" " 2		" "	5×10^{-4} radian
11	" " 3		" "	5×10^{-4} radian
12	" " 1		Random Drift	3×10^{-6} radian/sec
13	" " 2		" "	3×10^{-6} radian/sec
14	" " 3		" "	3×10^{-6} radian/sec
15	" " 1		"g-sensitive" drift	5×10^{-7} rad-sec/m
16	" " 2		" "	5×10^{-7} rad-sec/m
17	" " 3		" "	5×10^{-7} rad-sec/m
18	Clock Error			0 (See Note #2)

Note 1: A accelerometer alignment error is taken to be zero, as it is considered that the A accelerometer alignment defines a reference direction for all other alignments.

Note 2: Clock error was found to have a truly negligible effect even when using pessimistic estimates.

TABLE 2

NUMBER OF UNITS OF VARIANCE FOR ERROR SOURCES STUDIED

k	Description	90 Hr Lunar	66 Hr Lunar	42 Hr Lunar	118 Day Venus	88 Day Venus	235 Day Mars	216 Day Mars
1	A accelerometer scale factor error	18.100	20.139	27.207	32.466	17.565	45.431	14.142
2	B " " " "	9.867	5.211	5.736	18.411	14.118	9.124	11.555
3	A " null shift error	6.825	6.830	9.852	12.357	6.797	1.065	0.091
4	B " " " "	1.709	1.144	0.756	2.316	2.208	3.156	4.147
5	C " " " "	0.003	0.011	0.122	0.029	0.018	0.048	0.012
6	A " alignment error	0	0	0	0	0	0	0
7	B " " "	2.487	3.043	0.756	2.064	2.466	1.980	0.419
8	C " " "	0.008	0.027	0.287	0.062	0.038	0.103	0.026
9	Gyro No. 1 initial offset	7.102	6.719	2.707	7.965	6.175	3.761	3.640
10	" " 2 " " "	0.002	0.009	0.117	0.045	0.037	0.047	0.012
11	" " 3 " "	0.011	0.036	0.461	0.112	0.074	0.267	0.067
12	" " 1 random drift	6.637	8.412	21.343	1.507	7.557	5.761	2.655
13	" " 2 " "	0.000	0.002	0.479	0.350	0.367	0.782	0.213
14	" " 3 " "	0.030	0.080	1.115	0.203	0.112	2.294	0.543
15	" " 1 "g-sensitive" drift	47.154	48.160	25.992	21.106	41.627	24.632	62.084
16	" " 2 " "	0.001	0.012	0.528	0.451	0.415	0.223	0.064
17	" " 3 " "	0.062	0.165	2.542	0.556	0.427	1.327	0.329
18	Clock error	0	0	0	0	0	0	0
	TOTAL for all Sources	100.000	100.000	100.000	100.000	100.000	100.000	100.000
	TOTAL for Gyro No. 1	60.893	63.291	50.042	30.578	55.359	34.154	68.389
	TOTAL for A Accelerometer	24.925	26.969	37.059	44.823	24.362	46.496	14.233

The two totals shown above illustrate that one high quality accelerometer (A) and one high quality gyro (No. 1) would reduce uncorrected target errors significantly while improving the other components would have a much smaller effect.

TABLE 3

TRAJECTORY DESCRIPTION AND UNCORRECTED ONE-SIGMA

TARGET ERROR (FOM) DUE TO INJECTION ERRORS

Trajectory Number	Trajectory Type	Flight Time	Parking Orbit Interval (sec)	FOM(km)
1	Slow lunar	90 hrs	659.976	15,650.
2	Nominal lunar	66 hrs	721.648	6,380.
3	Fast lunar	42 hrs	859.978	2,530.
4	Slow Venus	118 days	784.3957	346,900.
5	Fast Venus	88 days	768.8225	212,100.
6	Slow Mars	235 days	1,575.6735	454,800.
7	Fast Mars	216 days	1,548.0000	351,300.

TABLE 4

STATISTICS OF INJECTION ERRORS FOR TRAJECTORY NO. 1[1]

Standard deviation

σ_x = 16.000 Km $\qquad$ ρ_{xr} = -0.86676

σ_r = 10.942 Km $\qquad$ ρ_{xv} = 0.98355

σ_v = 14.443 m/sec $\qquad$ $\rho_{x\Gamma}$ = -0.74795

σ_Γ = 2.0501 millirad $\quad$ ρ_{rv} = -0.91866

σ_z = 10.268 Km $\qquad$ $\rho_{r\Gamma}$ = 0.95163

$\sigma_{\dot{z}}$ = 18.255 m/sec $\qquad$ $\rho_{v\Gamma}$ = -0.81131

$\qquad\qquad\qquad\qquad\qquad$ $\rho_{z\dot{z}}$ = 0.40330

$\qquad\qquad\qquad\qquad\qquad$ $\rho_{xz} = \rho_{x\dot{z}} = \rho_{rz} = \rho_{r\dot{z}} = \rho_{vz} = \rho_{v\dot{z}} = \rho_{\Gamma z} = \rho_{\Gamma \dot{z}} = 0$

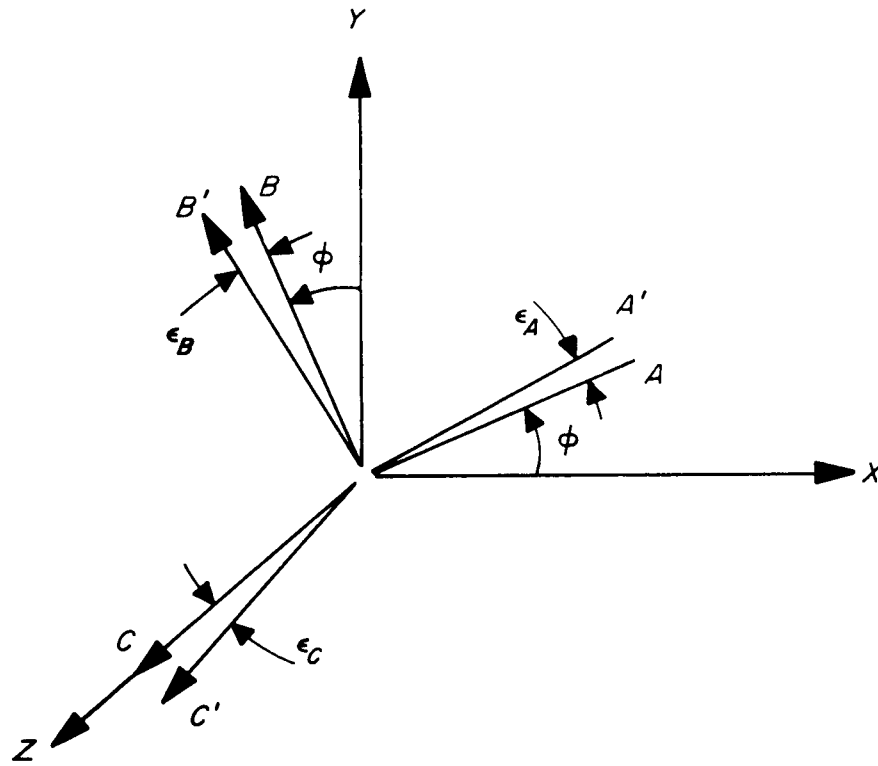[1] This data is representative of the seven trajectories studied.
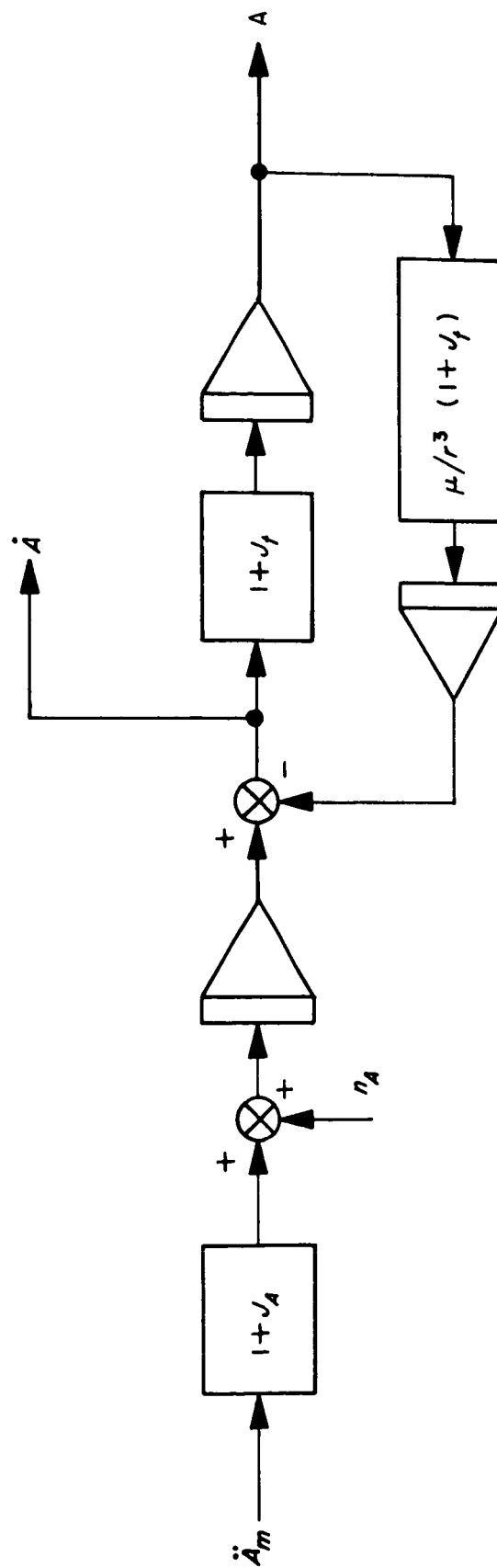
Fig. 1.   Accelerometer Orientation

Fig. 2. Accelerometer Computer Loop

IA – INPUT AXIS
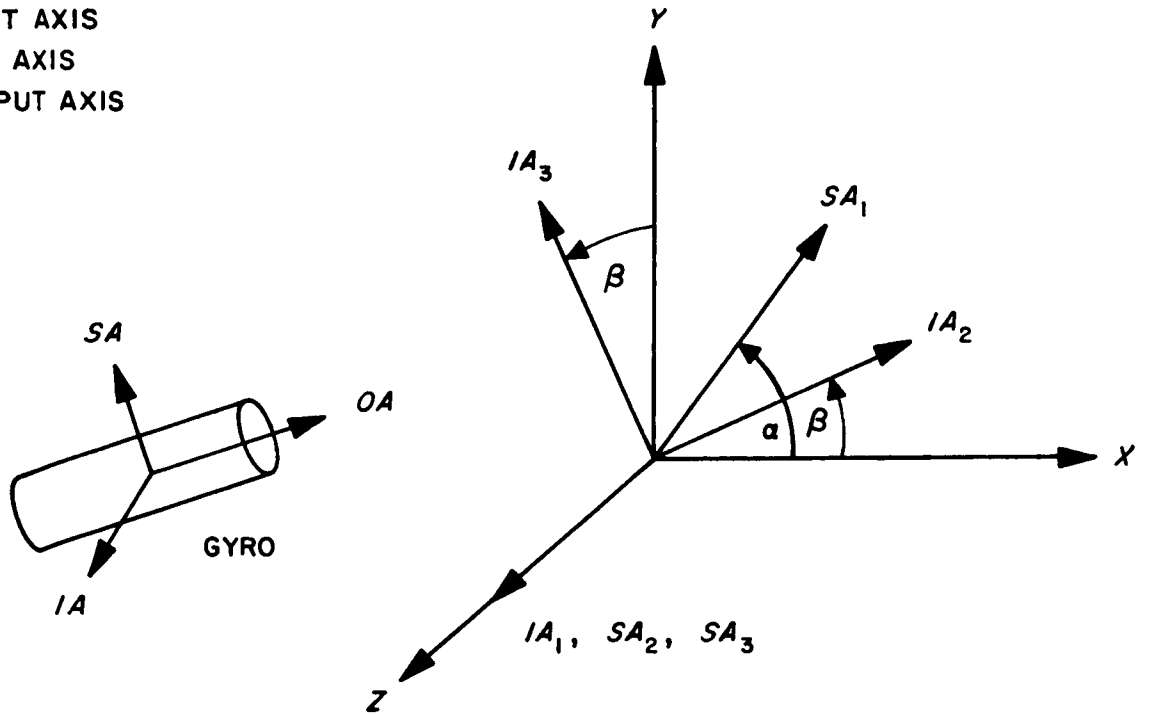SA – SPIN AXIS
OA – OUTPUT AXIS
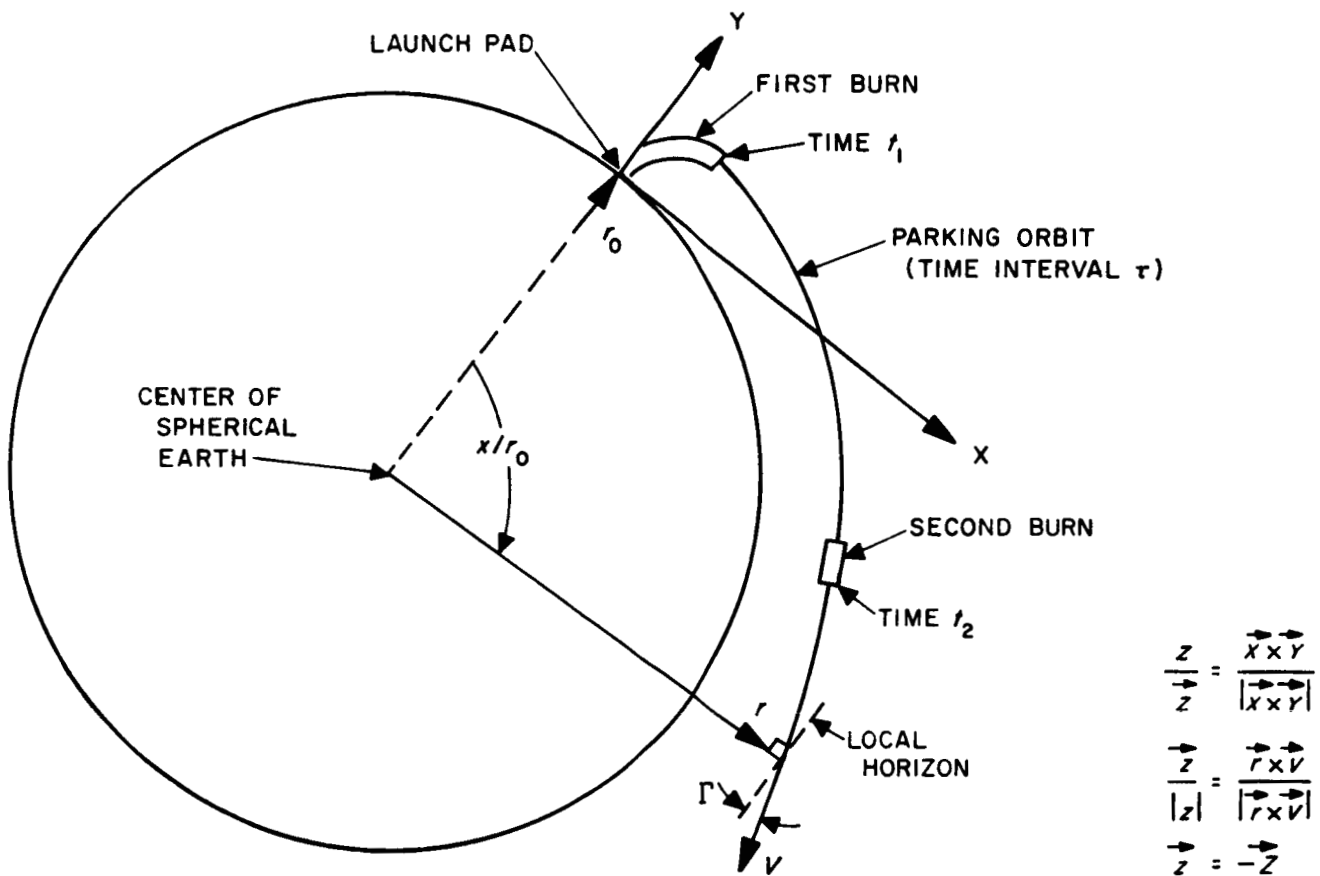
Fig. 3. Gyro Orientation
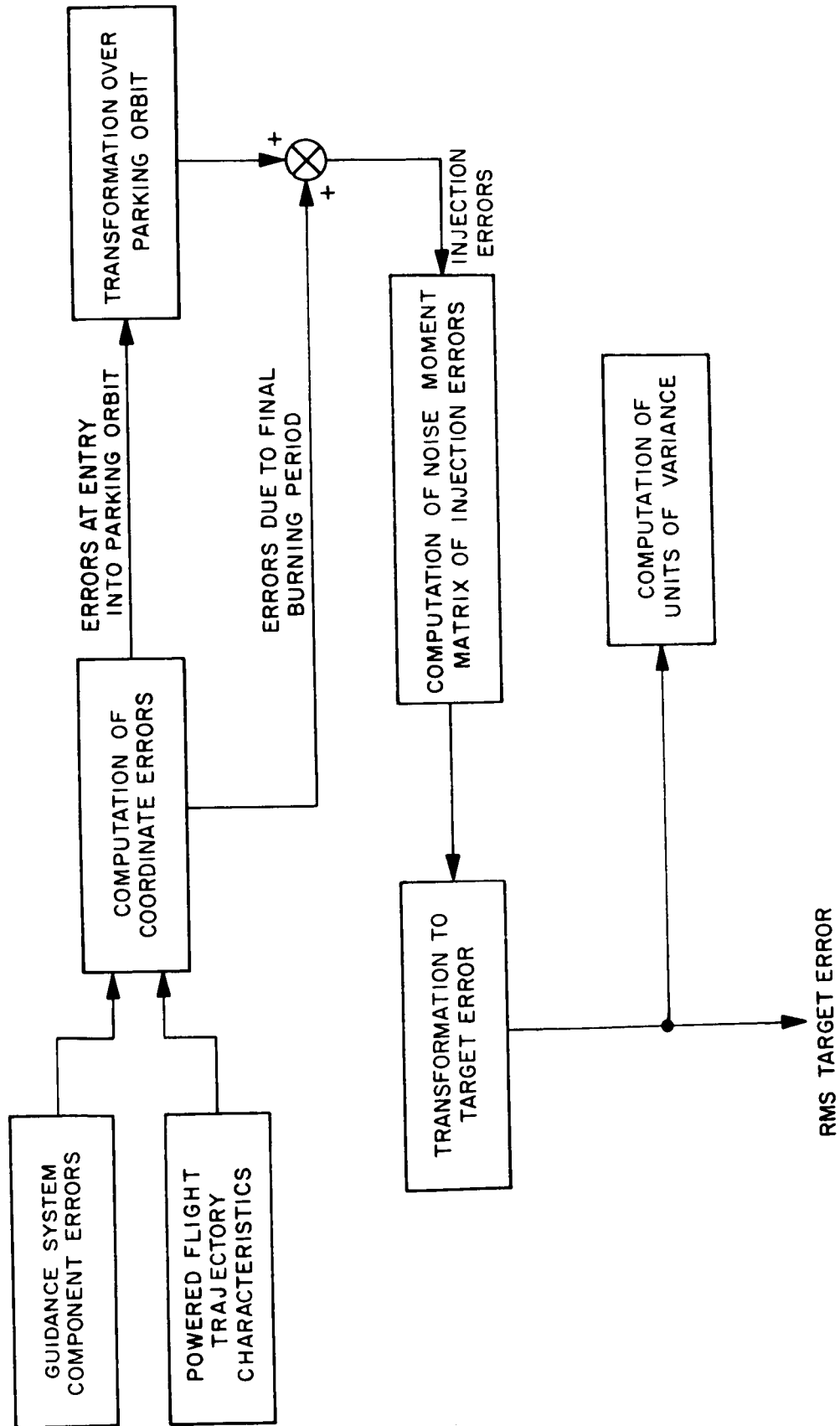
Fig. 4. Coordinate Systems
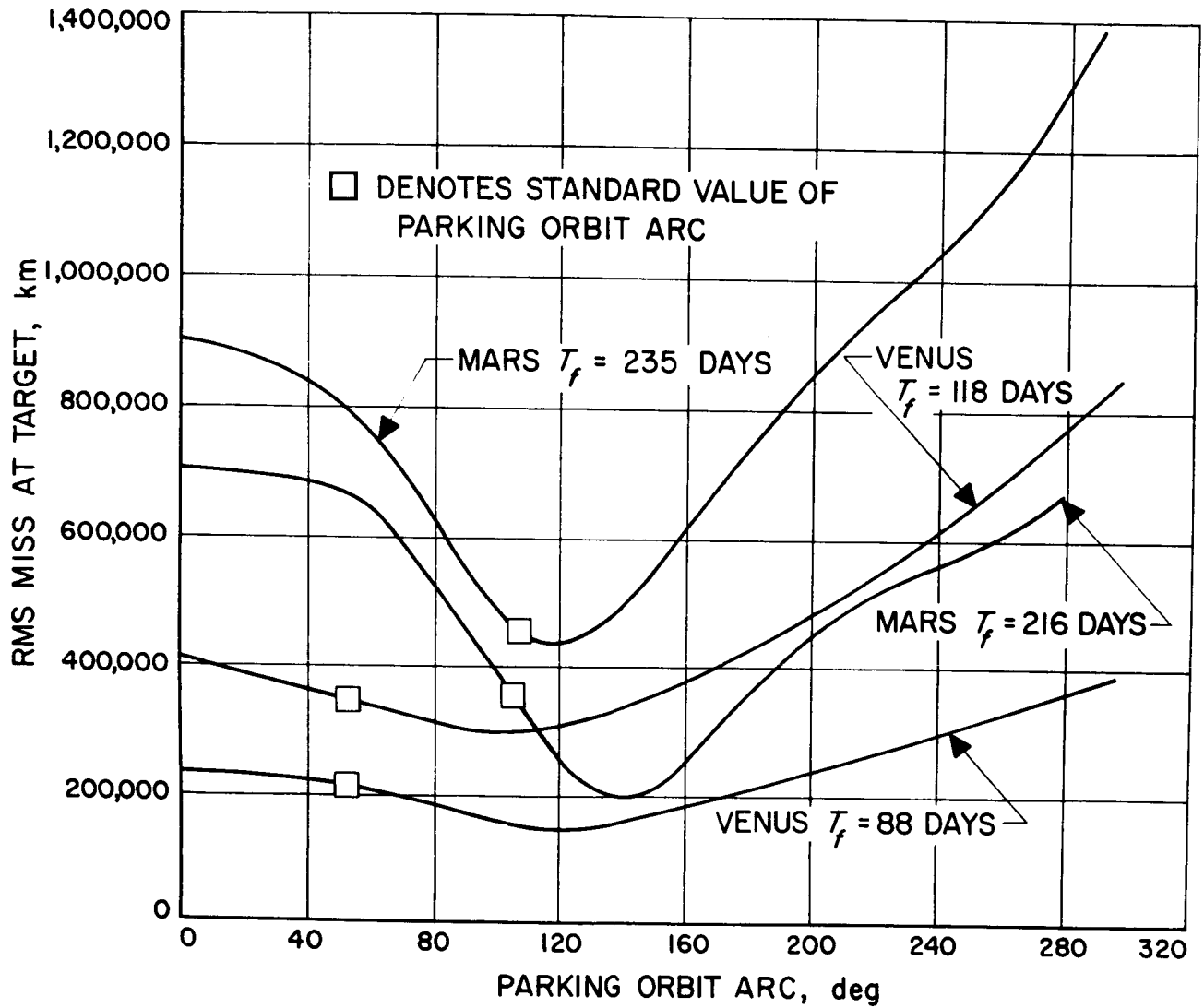
Fig. 5. Flow Chart of Error Study

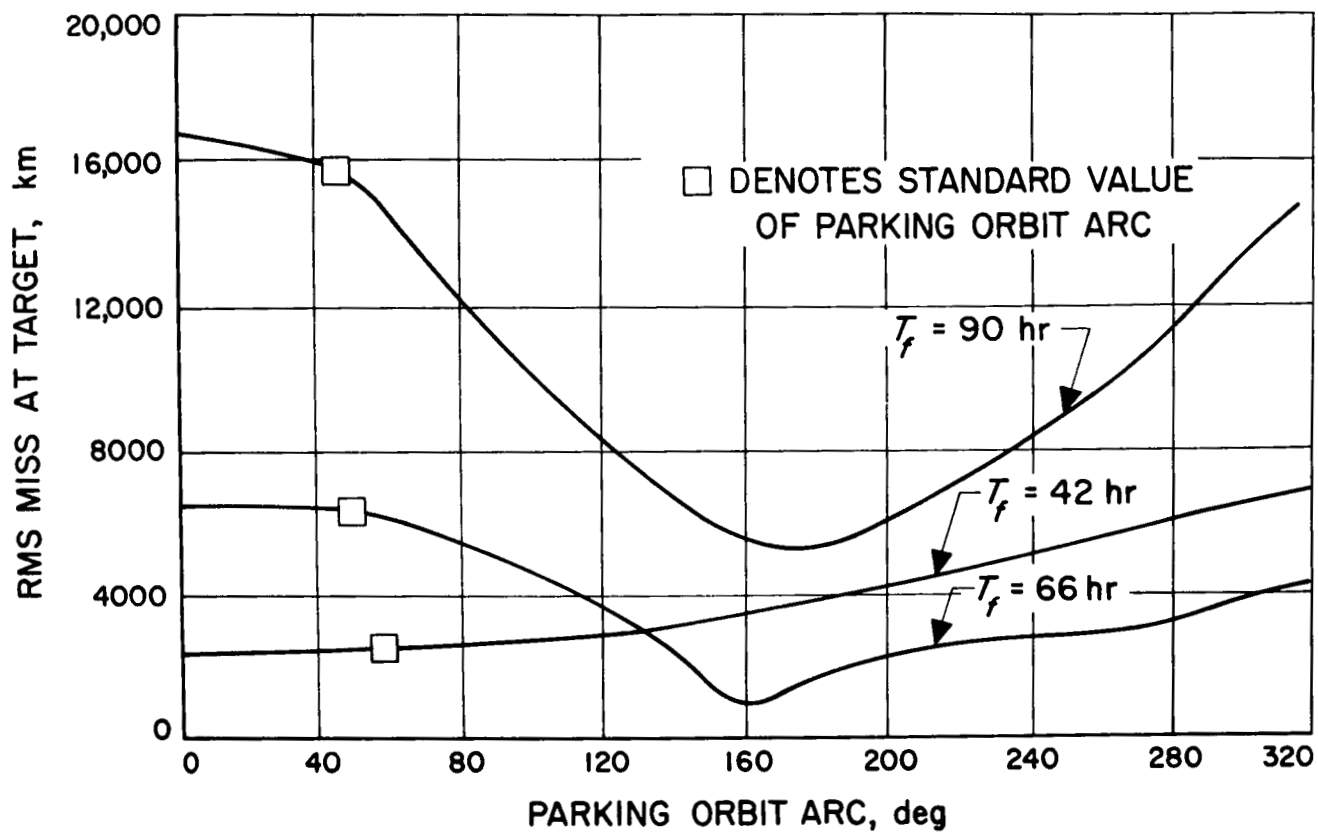Fig. 6. RMS Miss at Target vs Parking Orbit Arc for Typical Trajectories

Fig. 7. RMS Miss at Target vs Parking Orbit Arc for Typical Trajectories
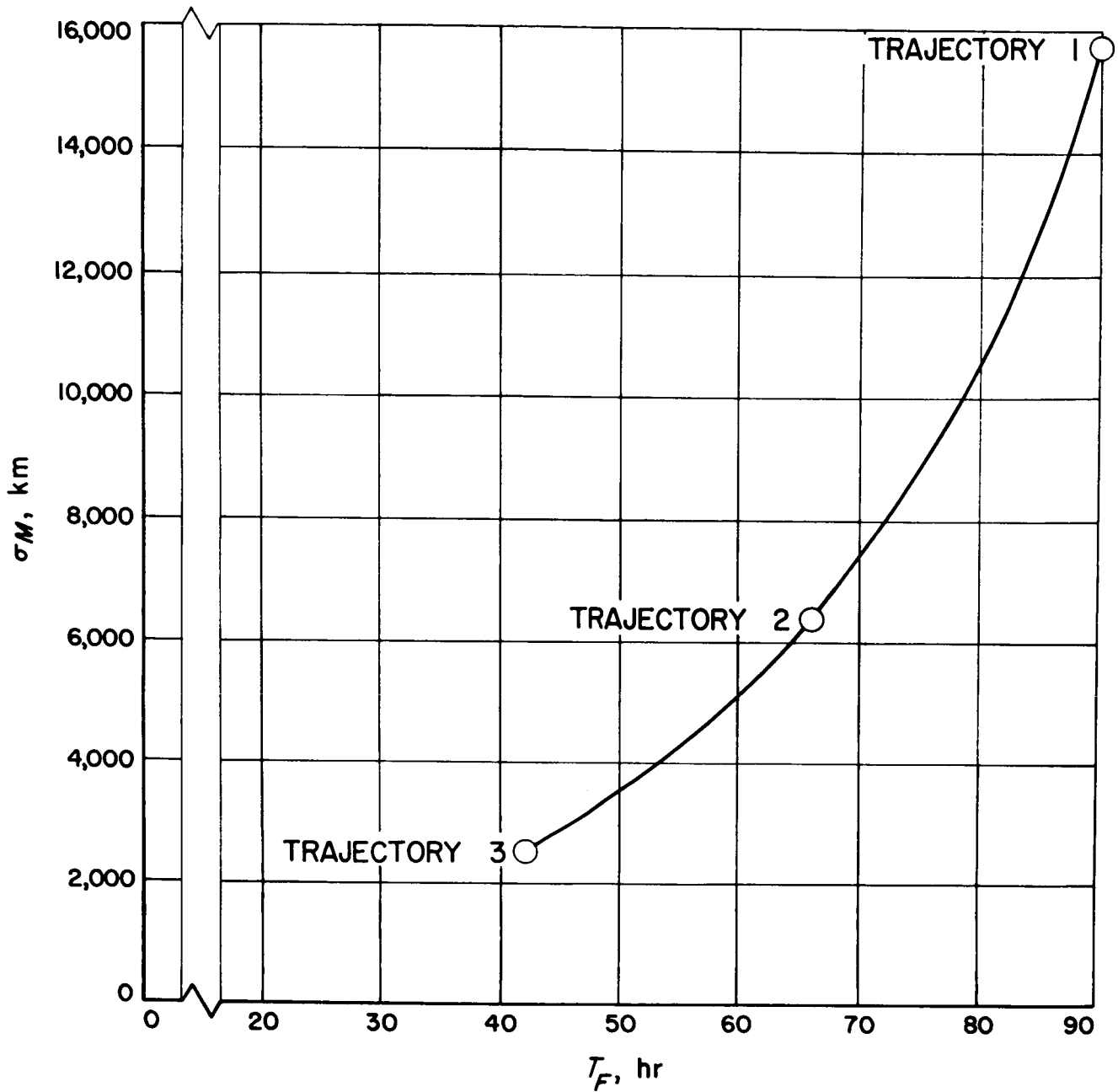
Fig. 8. RMS Target Miss vs Flight Time for Typical Lunar Trajectories
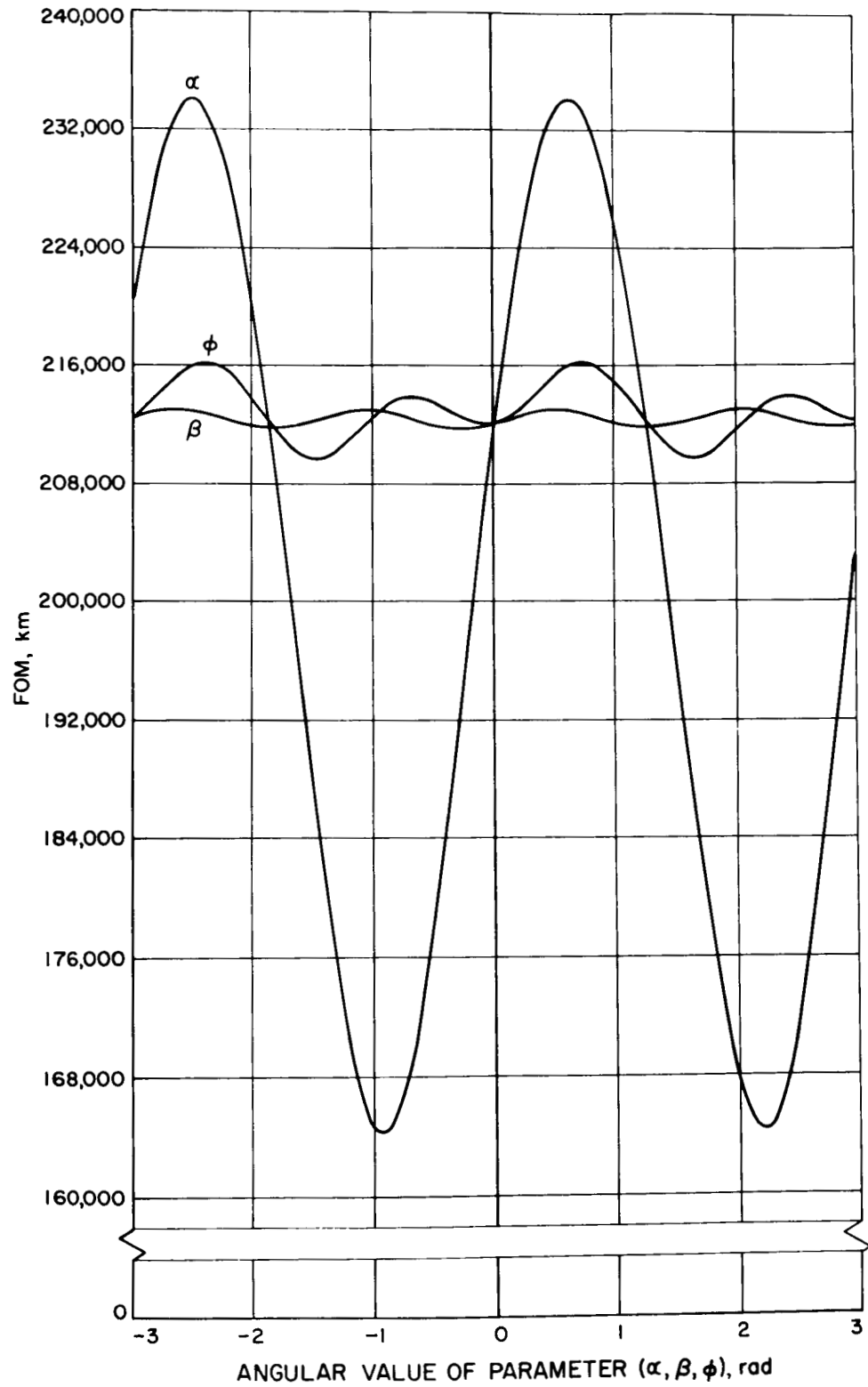
Fig. 9. RMS Target Error vs Value of Guidance Parameters for Trajectory No. 5

APPENDIX A

DESCRIPTION OF THE MATRICES

A. The B matrix - transforms errors in polar coordinates around the coast arc ψ.

$$
\begin{bmatrix}
1 & 0 & 0 & 0 & 0 & 0 \\[2ex]
\dfrac{r_0}{r}(2\sin\psi - 3\psi) & (2 - \cos\psi) & \dfrac{v}{r}(\cos\psi - 1) & \dfrac{\sin\psi}{r} & 0 & 0 \\[2ex]
\dfrac{r_0}{V}(4\sin\psi - 3\psi) & 2\dfrac{r}{v}(1 - \cos\psi) & (2\cos\psi - 1) & \dfrac{2\sin\psi}{v} & 0 & 0 \\[2ex]
2r_0(\cos\psi - 1) & r\sin\psi & -V\sin\psi & \cos\psi & 0 & 0 \\[2ex]
0 & 0 & 0 & 0 & \cos\psi & \dfrac{-v}{r}\sin\psi \\[2ex]
0 & 0 & 0 & 0 & \dfrac{r}{v}\sin\psi & \cos\psi
\end{bmatrix}
$$

$V = \sqrt{\dfrac{\mu}{r}}$ the circular satellite velocity at altitude $r - r_0$.

$r = \sqrt{X_1^2 + (y_1 + r_0)^2}$ the radial distance from the center of the Earth at injection into the parking orbit.

$\psi = (\Delta\tau + t_2 - t_1)\dfrac{V}{r}$ where $\Delta\tau$ is nominally zero and is used for arbitrarily changing the coast interval.

The values of r_0 and μ are:

	r_0	μ
English	20,902,910 ft	14.07689×10^{15} ft^3/sec^2
Metric	6,372,160 m	3.986135×10^{14} m^3/sec^2

B. The E_i matrix - transforms errors in Cartesian coordinates to errors in polar coordinates (i = 1 at end of first burn phase, i = 2 at end of second burn phase)

$$
\begin{bmatrix}
\dfrac{r_0}{r_i}\cos\left(\dfrac{x_i}{r_0}\right) & \sin\left(\dfrac{x_i}{r_0}\right) & 0 & \dfrac{1}{r_i}\cos\left(\dfrac{x_i}{r_0}\right) & 0 & 0 \\[2em]
-\dfrac{r_0}{r_i}\sin\left(\dfrac{x_i}{r_0}\right) & \cos\left(\dfrac{x_i}{r_0}\right) & 0 & -\dfrac{1}{r_i}\sin\left(\dfrac{x_i}{r_0}\right) & 0 & 0 \\[2em]
0 & 0 & \cos\left(\Gamma_i - \dfrac{x_i}{r_0}\right) & -\dfrac{1}{v}\sin\left(\Gamma_i - \dfrac{x_i}{r_0}\right) & 0 & 0 \\[2em]
0 & 0 & \sin\left(\Gamma_i - \dfrac{x_i}{r_0}\right) & \dfrac{1}{v}\cos\left(\Gamma_i - \dfrac{x_i}{r_0}\right) & 0 & 0 \\[2em]
0 & 0 & 0 & 0 & -1 & 0 \\[2em]
0 & 0 & 0 & 0 & 0 & -1
\end{bmatrix}
$$

$$r_i = \sqrt{X_i^2 + (Y_i + r_0)^2} \qquad \cos\left(\frac{x_i}{r_0}\right) = \frac{Y_i + r_0}{r_i} \qquad \cos\left(\Gamma_i - \frac{x_i}{r_0}\right) = \frac{\dot{X}_i}{V_i}$$

$$V_i = \sqrt{\dot{X}_i^2 + \dot{Y}_i^2} \qquad \sin\left(\frac{x_i}{r_0}\right) = \frac{X_i}{r_0} \qquad \sin\left(\Gamma_i - \frac{x_i}{r_0}\right) = \frac{\dot{Y}_i}{V_i}$$

The standard trajectory has all the necessary quantities in the inertial plumbline Cartesian coordinate system.

APPENDIX B

DERIVATION OF ERROR TERMS

One of the major aims of this analytical derivation is to avoid integrating perturbed trajectories. If the parking orbit interval is changed, the second burn phase produces different incremental Cartesian coordinates, although it produces identical incremental polar coordinates. (The incremental coordinates measured are of interest as they correspond to the physical situation of setting all initial conditions equal to zero at the start of the second burn.) With a changed parking orbit interval, the local horizon at start of second burn will have rotated through $V/r\Delta\tau$ radians with reference to the standard local horizon ($\Delta\tau = 0$). The effect of this rotation can be duplicated by imagining that the accelerometers and gyros have been rotated by this amount and that the second burn occurs at the standard location on the coast arc. Then the transformation $\left[\delta X\right]_2 E_2 = \left[\delta Z\right]_2$ uses the standard E_2 matrix. In the following derivations the subscript k takes values 1 or 2 for first or second burn, and $\xi_k = \xi + (k - 1)v/r\Delta\tau$, where ξ indicates $\emptyset$, α, or β.

A. Accelerometer Errors

1. Mathematical Model

Assume that the accelerometer axes A, B, C are aligned relative to a fixed inertial reference as shown in Fig. 1 and that the computer loop is as shown in Fig. 2.

2. Effect of an Accelerometer Scale Factor Error

From Fig. 2, the differential equation for the error in the A coordinate due to a scale factor error (J_A) only is:

$$\delta\ddot{A} + \frac{\mu}{r^3}\,\delta A = J_A\ddot{A}_m$$

The solution of this equation is

$$\delta A = J_A A = J_A\,(X\cos\emptyset + Y\sin\emptyset)$$

Therefore the error terms are[*]:

$$\delta\dot{X} = J_A(\dot{X}\cos^2\emptyset_k + \dot{Y}\sin\emptyset_k\cos\emptyset_k)$$

$$\delta X = J_A(X\cos^2\emptyset_k + Y\sin\emptyset_k\cos\emptyset_k)$$

$$\delta\dot{Y} = \delta\dot{X}\tan\emptyset_k$$

$$\delta Y = \delta X\tan\emptyset_k$$

$$\delta\dot{Z} = \delta Z = 0$$

Similarly for the B accelerometer:

---

[*]The subscript m denotes a measured coordinate, as distinguished from a true coordinate. It will be assumed throughout that the measured coordinate deviations are equal to the true coordinate deviations.

$$\delta\dot{X} = J_B(\dot{X} \sin^2 \phi_k - \dot{Y} \sin \phi_k \cos \phi_k)$$

$$\delta X = J_B(X \sin^2 \phi_k - Y \sin \phi_k \cos \phi_k)$$

$$\delta\dot{Y} = -\delta\dot{X} \cot \phi_k$$

$$\delta Y = -\delta X \cot \phi_k$$

and no first order errors arise from J_C.

3. Effect of a Null Shift Error

From Fig. 2, the differential equation for the error in A coordinates due to a null shift (n_A) only is:

$$\ddot{A} + \frac{\mu}{r^3} \delta A = n_A$$

The solution of this equation is

$$\delta A = n_A \frac{r^3}{\mu} \left[1 - \cos \left(\sqrt{\frac{\mu}{r^3}} t \right) \right]$$

Therefore the error terms are:

$$\delta\dot{X} = n_A \sqrt{\frac{r^3}{\mu}} \cos \phi_k \sin \left(\sqrt{\frac{\mu}{r^3}} t \right)$$

$$\delta X = n_A \frac{r^3}{\mu} \cos \phi_k \left[1 - \cos \left(\sqrt{\frac{\mu}{r^3}} t \right) \right]$$

$$\delta\dot{Y} = \delta\dot{X} \tan \phi_k$$

$$\delta Y = \delta X \tan \phi_k$$

$$\delta\dot{Z} = \delta Z = 0$$

Similarly for the B accelerometer:

$$\delta \dot{X} = -n_B \sqrt{\frac{r^3}{\mu}} \sin \phi_k \sin \left(\sqrt{\frac{\mu}{r^3}} t \right)$$

$$\delta X = -n_B \frac{r^3}{\mu} \sin \phi_k \left[1 - \cos \left(\sqrt{\frac{\mu}{r^3}} t \right) \right]$$

$$\delta \dot{Y} = -\delta \dot{X} \cot \phi_k$$

$$\delta Y = -\delta X \cot \phi_k$$

$$\delta \dot{Z} = \delta Z = 0$$

and for the C accelerometer:

$$\delta \dot{X} = \delta X = \delta \dot{Y} = \delta Y = 0$$

$$\delta \dot{Z} = n_C \sqrt{\frac{r^3}{\mu}} \sin \left(\sqrt{\frac{\mu}{r^3}} t \right)$$

$$\delta Z = n_C \frac{r^3}{\mu} \left[1 - \cos \left(\sqrt{\frac{\mu}{r^3}} t \right) \right]$$

4. Effect of an Alignment Error

From Fig. 1, looking at the A accelerometer only;

$$\ddot{A}_m = \ddot{X}_m \cos (\phi_k + \epsilon_A) + \ddot{Y}_m \sin (\phi_k + \epsilon_A)$$

so that, since ϵ_A is a small angle:

$$\delta \ddot{A}_m = \epsilon_A (-\ddot{X}_m \sin \phi_k + \ddot{Y}_m \cos \phi_k)$$

Therefore the error terms are:

$$\delta \dot{X} = \epsilon_A (-\dot{X}_m \sin \phi_k \cos \phi_k + \dot{Y}_m \cos^2 \phi_k)$$

$$\delta X = \epsilon_A (-X_m \sin \phi_k \cos \phi_k + Y_m \cos^2 \phi_k)$$

$$\delta \dot{Y} = \delta \dot{X} \tan \phi_k$$

$$\delta Y = \delta X \tan \phi_k$$

$$\delta \dot{Z} = \delta Z = 0$$

Similarly for the B accelerometer:

$$\delta \dot{X} = \epsilon_B (\dot{X}_m \cos \phi_k \sin \phi_k + \dot{Y}_m \sin^2 \phi_k)$$

$$\delta X = \epsilon_B (X_m \cos \phi_k \sin \phi_k + Y_m \sin^2 \phi_k)$$

$$\delta \dot{Y} = -\delta \dot{X} \cot \phi_k$$

$$\delta Y = -\delta X \cot \phi_k$$

$$\delta \dot{Z} = \delta Z = 0$$

The C accelerometer alignment error was considered to consist of two components, ϵ_{CX} and ϵ_{CY} such that:

$$\delta \ddot{Z} = \epsilon_{CX} \ddot{X}_m + \epsilon_{CY} \ddot{Y}_m$$

Assuming that these two components are uncorrelated and have equal standard deviations, ϵ_C, about zero mean;

$$\sigma_{\dot{Z}}^2 = \epsilon_C^2 (\dot{X}_m^2 + \dot{Y}_m^2)$$

Therefore the error terms are:

$$\delta\dot{Z} = \epsilon_C \sqrt{\dot{X}_m^2 + \dot{Y}_m^2}$$

$$\delta Z = \epsilon_C \sqrt{X_m^2 + Y_m^2}$$

$$\delta\dot{X} = \delta X = \delta\dot{Y} = \delta Y = 0$$

5. Effect of Integrator Scale Factor Error (Clock Error)

This error arises from errors in the timing device that controls the integration interval in the digital integrator. From Fig. 2, the differential equation for the error in A coordinates due to a clock error (J_t) only is:

$$\delta\ddot{A} + (1 + J_t)^2 \frac{\mu}{r^3} \delta A = (2 + J_t) J_t \ddot{A} - (1 + J_t) J_t \ddot{A}_m$$

The solution of this equation is:

$$\delta A = J_t \cos\left(\sqrt{\frac{\mu}{r^3}} t\right) \int \sec^2\left(\sqrt{\frac{\mu}{r^3}} T\right) \int (2\ddot{A} - \ddot{A}_m) \cos\left(\sqrt{\frac{\mu}{r^3}} \tau\right) d\tau dT$$

$$= J_t (2A - A_m) \text{ to first order}^*$$

$$\delta\dot{A} = J_t (\dot{A} - \dot{A}_m) \text{ to first order}^*$$

---

*Although all the terms required to evaluate the integrals are available on the standard trajectory, it was found that the first order approximation is quite adequate for these terms.

Therefore the error terms are:

$$\delta\dot{X} = J_t(\dot{X} - \dot{X}_m)$$

$$\delta X = J_t(2X - X_m)$$

$$\delta\dot{Y} = J_t(\dot{Y} - \dot{Y}_m)$$

$$\delta Y = J_t(2Y - Y_m)$$

$$\delta\dot{Z} = \delta Z = 0$$

The clock error would also cause a change in the parking orbit interval. This effect, which is that of starting the second burn at the wrong time can be most easily calculated directly in polar coordinates. It is simply an error in the downrange distance:

$$\delta x = -J_t r_0 \frac{V}{r}(t_1 + \tau + \Delta\tau)$$

where τ is the parking orbit interval. This element forms the only non-zero element in $[\delta Z]_3$.

B. Gyro Errors

1. Mathematical Model

Assume that the gyro axes are oriented as shown in Fig. 3. This particular configuration is chosen so as to eliminate anisoelastic drift rate (i.e., drift rate proportional to the product of accelerations along spin

and input axes) while maintaining orthogonality of the input axes. With no anisoelastic drift, the general expression for angular error, θ, about the input axis of a gyro is:

$$\theta = \theta_0 + \dot{\theta}_0 t + \mu_S \int a_I dt - \mu_I \int a_S dt$$

θ_0 is the initial offset

$\dot{\theta}_0$ is the random drift rate

a_I is the measurable acceleration along the input axis

a_S is the measurable acceleration along the spin axis

μ_I and μ_S are constants

The gyro error will cause the accelerometers to sense a false acceleration, the acceleration error vector being:

$$\vec{\delta a} = \vec{\theta} \times \vec{a}_m \text{ (standard)} = \begin{vmatrix} \vec{i} & \vec{j} & \vec{k} \\ \theta_1 & \theta_2 & \theta_3 \\ \ddot{X}_m & \ddot{Y}_m & 0 \end{vmatrix}$$

2. Input axis perpendicular to the thrust plane (IA_1)

$$\vec{\delta a} = \begin{vmatrix} \vec{i} & \vec{j} & \vec{k} \\ 0 & 0 & \theta \\ X_m & Y_m & 0 \end{vmatrix} = \vec{j}\theta\ddot{X}_m - \vec{i}\,\theta\,\ddot{Y}_m$$

$$\delta \ddot{X} = -\ddot{Y}_m \theta = -\ddot{Y}_m \theta_0 + \dot{\theta}_0 t - \mu_I \int_0^t (\ddot{X}_m \cos \alpha + \ddot{Y}_m \sin \alpha) \, dt$$

$$\delta \ddot{Y} = \ddot{X}_m \theta = \ddot{X}_m \left[\theta_0 + \dot{\theta}_0 t - \mu_I \int_0^t (\ddot{X}_m \cos \alpha + \ddot{Y}_m \sin \alpha) \, dt \right]$$

The integral appearing in these two equations must be evaluated as:

$$(k - 1)(\dot{X}_{m1} \cos \alpha_1 + \dot{Y}_{m1} \sin \alpha_1) + \int_{t_{k-1}}^{t_k} (\ddot{X}_m \cos \alpha_k + \ddot{Y}_m \sin \alpha_k) \, dt$$

where the quantities multiplied by (k - 1) represent the "g-sensitive" drift effects of first burn as initial conditions for the second burn. Setting this quantity, $\dot{X}_{m_1} \cos \alpha_1 + \dot{Y}_{m_1} \sin \alpha_1 = W_1$, and interpreting the integral to be over the first or second burning phase (for k = 1 or 2 respectively), the error terms are:

$$\delta \dot{X} = -\theta_0 \dot{Y}_{mk} - \dot{\theta}_0 \left[\dot{I}_{1k} + (k - 1) \dot{Y}_{m2} (t_1 + \tau + \Delta \tau) \right]$$

$$+ \mu_I \left[\dot{I}_{3k} \cos \alpha_k + \dot{I}_{4k} \sin \alpha_k + (k - 1) \dot{Y}_{m2} W_1 \right]$$

$$\delta X = -\theta_0 Y_{mk} - \dot{\theta}_0 \left[I_{1k} + (k - 1) Y_{m2} (t_1 + \tau + \Delta \tau) \right]$$

$$+ \mu_I \left[I_{3k} \cos \alpha_k + I_{4k} \sin \alpha_k + (k - 1) Y_{m2} W_1 \right]$$

$$\delta \dot{Y} = \theta_0 \dot{X}_{mk} + \dot{\theta}_0 \left[\dot{I}_{2k} + (k - 1) \dot{X}_{m2} (t_1 + \tau + \Delta \tau) \right]$$

$$- \mu_I \left[\dot{I}_{5k} \cos \alpha_k + \dot{I}_{6k} \sin \alpha_k + (k - 1) \dot{X}_{m2} W_1 \right]$$

$$\delta Y = \theta_0 X_{mk} + \dot{\theta}_0 \left[I_{2k} + (k - 1) X_{m2}(t_1 + \tau + \Delta\tau) \right]$$

$$- \mu_I \left[I_{5k} \cos\alpha_k + I_{6k} \sin\alpha_k + (k - 1) X_{m2} W_1 \right]$$

$$\delta\dot{Z} = \delta Z = 0$$

where

$$\dot{I}_{1k} = \int_{t_{k-1}}^{t_k} (t - t_{k-1}) \ddot{Y}_m dt \qquad I_{1k} = \iint_{t_{k-1}}^{t_k} (t - t_{k-1}) \ddot{Y}_m dt^2$$

$$\dot{I}_{2k} = \int_{t_{k-1}}^{t_k} (t - t_{k-1}) \ddot{X}_m dt \qquad I_{2k} = \iint_{t_{k-1}}^{t_k} (t - t_{k-1}) \ddot{X}_m dt^2$$

$$\dot{I}_{3k} = \int_{t_{k-1}}^{t_k} \ddot{Y}_m \dot{X}_m dt \qquad I_{3k} = \iint_{t_{k-1}}^{t_k} \ddot{Y}_m \dot{X}_m dt^2$$

$$\dot{I}_{4k} = \int_{t_{k-1}}^{t_k} \ddot{Y}_m \dot{Y}_m dt \qquad I_{4k} = \iint_{t_{k-1}}^{t_k} \ddot{Y}_m \dot{Y}_m dt^2$$

$$\dot{I}_{5k} = \int_{t_{k-1}}^{t_k} \ddot{X}_m \dot{X}_m dt \qquad I_{5k} = \iint_{t_{k-1}}^{t_k} \ddot{X}_m \dot{X}_m dt$$

$$\dot{I}_{6k} = \int_{t_{k-1}}^{t_k} \ddot{X}_m \dot{Y}_m dt \qquad I_{6k} = \iint_{t_{k-1}}^{t_k} \ddot{X}_m \dot{Y}_m dt^2$$

3. Spin Axis Perpendicular to the Thrust Plane (SA_2, SA_3).

Consider gyro No. 2, where the input axis is β degrees above the X axis (the analysis for gyro No. 3 follows immediately by setting $\beta' = \beta + 90°$).

$$\vec{\delta a} = \begin{vmatrix} \vec{i} & \vec{j} & \vec{k} \\ \theta\cos\beta_k & \theta\sin\beta_k & 0 \\ \ddot{X}_m & \ddot{Y}_m & 0 \end{vmatrix} = \vec{k}\,\theta(\ddot{Y}_m\cos\beta_k - \ddot{X}_m\sin\beta_k)$$

$$\delta\ddot{Z} = \theta_0(\ddot{Y}_m\cos\beta_k - \ddot{X}_m\sin\beta_k) + \dot{\theta}_0 t(\ddot{Y}_m\cos\beta_k - \ddot{X}_m\sin\beta_k)$$

$$+ \mu_S(\ddot{Y}_m\cos\beta_k - \ddot{X}_m\sin\beta_k)\int_0^t (\ddot{X}_m\cos\beta + \ddot{Y}_m\sin\beta)\,dt$$

As in Part 2 of this Appendix, the integral must be evaluated as:

$$(k - 1)(\dot{X}_{m1}\cos\beta_1 + \dot{Y}_{m1}\sin\beta_1) + \int_{t_{k-1}}^{t_k} (\ddot{X}_m\cos\beta_k + \ddot{Y}_m\sin\beta_k)\,dt$$

where the quantities multiplied by (k - 1) represent the "g-sensitive" drift effects of first burn as initial conditions for the second burn. Setting this quantity, $\dot{X}_{m1}\cos\beta_1 + \dot{Y}_{m1}\sin\beta_1 = W_2$, the error terms are:

$$\delta\dot{X} = \delta X = \delta\dot{Y} = \delta Y = 0$$

$$\delta \dot{Z} = \theta_0 (\dot{Y}_{mk} \cos \beta_k - \dot{X}_{mk} \sin \beta_k) + \dot{\theta}_0 \Big[\dot{I}_{1k} \cos \beta_k - \dot{I}_{2k} \sin \beta_k +$$

$$(k - 1)(\dot{Y}_{m2} \cos \beta_2 - \dot{X}_{m2} \sin \beta_2)(t_1 + \tau + \Delta \tau) \Big]$$

$$+ \mu_S \Big[\dot{I}_{3k} \cos^2 \beta_k + (\dot{I}_{4k} - \dot{I}_{5k}) \cos \beta_k \sin \beta_k - \dot{I}_{6k} \sin^2 \beta_k +$$

$$(k - 1)(\dot{Y}_{m2} \cos \beta_2 - \dot{X}_{m2} \sin \beta_2) W_2 \Big]$$

$$\delta Z = \theta_0 (Y_{mk} \cos \beta_k - X_{mk} \sin \beta_k) + \dot{\theta}_0 \Big[I_{1k} \cos \beta_k - I_{2k} \sin \beta_k +$$

$$(k - 1)(Y_{m2} \cos \beta_2 - X_{m2} \sin \beta_2)(t_1 + \tau + \Delta \tau) \Big]$$

$$+ \mu_S \Big[I_{3k} \cos^2 \beta_k + (I_{4k} - I_{5k}) \cos \beta_k \sin \beta_k - I_{6k} \sin^2 \beta_k +$$

$$(k - 1)(Y_{m2} \cos \beta_2 - X_{m2} \sin \beta_2) W_2 \Big]$$

The twelve integrals used in the above analysis can be reduced to seven, since, after integration by parts:

$$\dot{I}_{1k} = \dot{Y}_{mk}(t_k - t_{k-1}) - Y_{mk}$$

$$I_{1k} = Y_{mk}(t_k - t_{k-1}) - 2I_{7k}$$

where

$$I_{7k} = \int_{t_{k-1}}^{t_k} Y_m dt$$

$$\dot{I}_{2k} = \dot{X}_{mk}(t_k - t_{k-1}) - X_{mk}$$

$$I_{2k} = X_{mk}(t_k - t_{k-1}) - 2I_{8k}$$

where

$$I_{8k} = \int_{t_{k-1}}^{t_k} X_m dt$$

$$I_{3k} = \dot{I}_{3k}(t_k - t_{k-1}) - I_{9k}$$

where

$$I_{9k} = \int_{t_{k-1}}^{t_k} (t - t_{k-1})\ddot{Y}_m\dot{X}_m dt$$

$$\dot{I}_{4k} = \frac{1}{2}\dot{Y}_{mk}^2$$

$$I_{4k} = \frac{1}{2}I_{10k}$$

where

$$I_{10k} = \int_{t_{k-1}}^{t_k} \dot{Y}_m^2 dt$$

$$\dot{I}_{5k} = \frac{1}{2}\dot{X}_{mk}^2$$

$$I_{5k} = \frac{1}{2}I_{11k}$$

where

$$I_{11k} = \int_{t_{k-1}}^{t_k} \dot{X}_m^2 dt$$

$$\dot{I}_{6k} = \dot{Y}_{mk}\dot{X}_{mk} - \dot{I}_{3k}$$

$$I_{6k} = I_{12k} - I_{3k}$$

where

$$I_{12k} = \int_{t_{k-1}}^{t_k} \dot{Y}_m \dot{X}_m \, dt$$

Thus the integrals $\dot{I}_{3k}$, I_{7k}, I_{8k}, I_{9k}, I_{10k}, I_{11k}, and I_{12k} are needed, and these can be evaluated in terms of quantities available on the standard trajectory.

REFERENCES

1. An Introduction to the Operation and Testing of Accelerometers by G. W. Meisenholder, Jet Propulsion Laboratory, CIT, TM 33-2 October 3, 1960.

2. Evaluation of Precision Gyros for Space Boost Guidance Applications by L. K. Jensen, B. H. Evans and R. B. Clark of Space Technology Laboratory, Los Angeles, Calif., presented at the American Rocket Society Semi-Annual Meeting, May 9-12, 1960 (ARS 1175-60).

3. Preliminary Descriptive Material on the GG8001 B Miniature Integrating Gyro, Minneapolis Honeywell, Aeronautical Division, U-ED 9841, March 28, 1960.

4. Preliminary Descriptive Document, GG177 Hinged Pendulous Accelerometer, Minneapolis Honeywell, Aeronautical Division, U-ED 9870, October 6, 1960.

5. The Statistical Analysis of Space Guidance Systems by A. R. M. Noton, Jet Propulsion Laboratory, CIT, TM 33-15, June 15, 1960.

6. Analysis of Radio-Command Mid-Course Guidance by A. R. M. Noton, E. Cutting and F. L. Barnes, Jet Propulsion Laboratory, CIT, TR 32-28, September 8, 1960.

7. A Method of Describing Miss Distances for Lunar and Interplanetary Trajectories by W. Kizner, Jet Propulsion Laboratory, CIT, EP 674, August 1, 1959.

8. Design of Lunar and Interplanetary Ascent Trajectories by V. C. Clarke, Jr., Jet Propulsion Laboratory, CIT, TR 32-30, July 26, 1960.